Generalized dynamic domain shape calculation in ferroelectric liquid crystals

Qi Jiang, Joseph E. Maclennan, and Noel A. Clark
Condensed Matter Laboratory, Department of Physics, University of Colorado, Boulder, Colorado 80309
(Received 2 November 1995)

We have developed an analytical algorithm analogous to the Wulff construction for calculating the spatial evolution of growing two-dimensinal (2D) domains as a function of time for arbitrary starting shapes. Applying the method to polarization domain growth in surface-stabilized ferroelectric liquid crystals, we can derive the full 2D shapes of polarization domains with curved walls from the directional variation of the velocity of planar walls as measured by computer simulations in only 1D. It is shown that the domain shape is determined in the present model by the anisotropic nematic elastic properties of the material. [S1063-651X(96)07606-4]

PACS number(s): 61.30.Cz, 83.70.Jr, 77.80.Fm

I. INTRODUCTION

The shapes of domains growing in condensed systems can tell us much about the underlying physics of the phases involved [1]. Examples include crystallization from solute or melt, directional solidification, and the growth of one liquid crystal phase or orientation in another. Domain growth is typically driven by temperature or density gradients, changes in pressure, or external fields, and the observed morphology may be a function of kinetic factors or of such static properties as surface energy anisotropy, surface tension, and bulk elasticity.

Such domains are typically multidimensional (d-dimensional) objects bounded by localized $(d-1)$-dimensional interfaces. In general, modeling of the domain shape requires calculation or simulation of the interface surface and profile in d dimensions. This paper deals with conditions under which the understanding and modeling of domain shape can be greatly simplified. Specifically we consider the situation in which (a) the interface thickness is small in comparison to its radius of curvature, and (b) the local velocity of interface advance, $v_n(\hat{\mathbf{n}})\hat{\mathbf{n}}$, depends *only* on the instantaneous orientation of the local interface unit normal, $\hat{\mathbf{n}}$, i.e., is independent of its curvature, history, and the location of other interface elements. Condition (b) implies that $v_n(\hat{\mathbf{n}})\hat{\mathbf{n}}$ would be the steady state velocity of a planar interface traveling in the direction $\hat{\mathbf{n}}$. We show that the domain shape can be obtained from $v_n(\hat{\mathbf{n}})$ in a way analogous to the Wulff construction [2], which relates equilibrium crystal shape to the dependence of the interfacial tension $\gamma(\hat{\mathbf{n}})$ on surface orientation, $\hat{\mathbf{n}}$. Since the calculation of $v_n(\hat{\mathbf{n}})\hat{\mathbf{n}}$ for a planar interface is a one-dimensional problem, the modeling of domain shape is reduced to the one-dimensional (1D) solution for the propagation of a planar interface vs orientation $\hat{\mathbf{n}}$.

We apply this technique to calculate the shape evolution of polarization domains in surface-stabilized ferroelectric liquid crystal (SSFLC) cells driven by applied electric fields. SSFLC cells typically contain chiral smectic-C (Sm-C) liquid crystal, which exhibits a spontaneous polarization normal to the molecular tilt plane [3]. The smectic layers are oriented approximately perpendicular to the conductive bounding plates, a geometry which forms the basis of fast electro-optic devices [4]. In general, the optical response of SSFLC's to applied electric fields is a complex function of the cell thickness, the voltage, and the material parameters of the liquid crystal. In particular, in cells with the chevron layer structure [5] sketched in Fig. 1(a), the direction of the ferroelectric polarization at the chevron interface can be switched between UP and DOWN by relatively weak fields ($E\sim$ a few V/μm). This local reorientation couples elastically to the dipoles in the rest of the cell, as shown in Fig. 1(b) [6]. Since the ferroelectric dipoles are rigidly connected to the molecular orientation, polarization reversal causes large changes in the optical transmission when the cells are suitably oriented between crossed polarizers [7].

The electro-optic response of chevron SSFLC's is mainly determined by the polarization switching at the chevron interface. This process typically involves the nucleation and subsequent growth of many individual, switched domains of high optical contrast [8,9]. In the two-dimensional (2D) view afforded by the polarizing microscope, these domains exhibit a variety of interesting and complicated morphologies, ranging from polygonal in low applied fields to almost elliptical in high fields. Since the dynamics of domain growth (which we modeled in our previous paper [10]) directly determines the electro-optic preformance of SSFLC's, there are clear practical incentives for studying this phenomenon.

This paper is arranged as follows. After reviewing the basic principles of the Wulff construction in the following section, we will describe our generalized method for calculating dynamic domain shapes and apply it to the specific case of SSFLC's. We conclude by addressing the feasibility of inferring physical parameters from observed domain shapes.

II. MOTIVATION

The Wulff construction is an appealingly simple way of deriving the *equilibrium* shapes of crystals when the angular dependence of the surface energy anisotropy $\gamma(\beta)$ is known, with β being the angle between $\mathbf{n}$, the unit normal to the domain wall, and the y axis, as shown in Fig. 2. The crystal shape corresponds to the minimal area enclosed by the set of lines drawn through each point of the energy surface, such that each line is oriented normal to the ''radial'' vector joining the center of the $\gamma(\beta)$ plot to that point. An extensive review and general proof of the validity of the Wulff con-

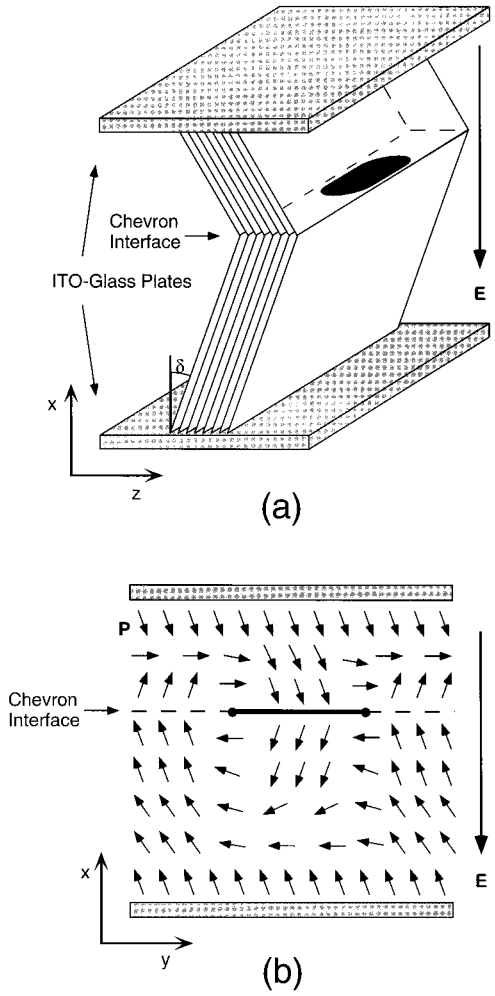

FIG. 1. (a) Geometry of chevron SSFLC cell. The smectic layers are tilted an angle $\pm\delta$ from the cell normal, forming a chevron-like structure. A generic domain (in black) is shown growing along the planar chevron interface. (b) Polarization domain switching at the chevron interface. A DOWN domain is shown growing in an UP environment, the arrows representing the polarization field **P**. This is a transverse view of the cell shown in (a), with the chevron domain boundaries indicated by the filled circles (●).

struction has been given by Herring [11].

In this paper we have developed an analysis comparable to the Wulff construction that allows us to determine *non-equilibrium* steady-state shapes of domains or crystals when the domain wall velocity as a function of surface orientation $v_n(\beta)$ is known. Our results confirm an observation, also attributed to Wulff, which is that fast-growing faces are soon eliminated from any crystal, while slow-growing faces persist and eventually dominate the crystal shape. While the Wulff construction gives the final (equilibrium) shape of crystals, our analytic recipe, which basically involves advancing each (infinitesimal) segment of the domain wall by an amount proportional to the speed of a 1D wall with the same orientation, enables us to compute the (nonequilibrium) evolution of domains of arbitrary starting shape as a function of time. We assume that a single kinetic quantity, such as the velocity $v_n(\beta)$, can completely describe the evolution of the domain shape.

Although the analysis is quite general, our specific interest is in explaining the shape of polarization domains in SSFLC's [12]. Recent experimental observations have shown that the growth at measurable times is self-similar, implying that the steady-state velocity along a given direction is constant in time [9].

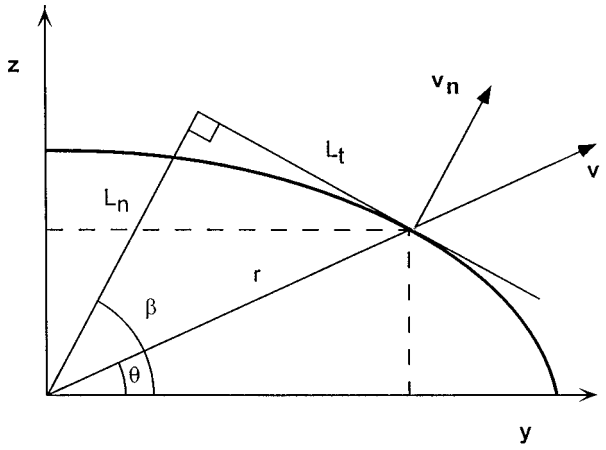

FIG. 2. Geometry of domain shape calculations. The curved domain boundary advances with velocity v and the normal component is given by v_n.

For the growth model used in this paper, we show that in the simplest mathematical description of SSFLC switching the angular dependence of growth velocity $v_n(\beta)$ is determined primarily by the nematic elastic anisotropy of the liquid crystal. The equilibrium shape of the domain therefore closely depends on the inherent properties of the material. In our simple model, we consider the applied field as the only driving force for domain growth. We find that the field only scales the magnitude of the velocity $v_n(\beta)$, whereas we have observed in experiments that changing the field may also lead to fundamental changes in the symmetry of the observed domain shapes. We also note that we are considering purely deterministic systems, where thermal fluctuation effects on the growth morphology can be ignored. The formalism is presented in the following section.

III. CALCULATION OF THE SHAPES OF GROWING DOMAINS

The following general algorithm for calculating the (nonequilibrium) steady-state shape of switching domains uses the normal velocity profile $v_n(\beta)$ of the domain boundaries, assumed to be independent of time t. This is consistent with the experimental observation that the mean dimension of switching domains in chevron SSFLC cells increases linearly with time [9]. Under conditions of stable growth, therefore, the domain wall velocity $v(\theta)$ is independent of r along any given direction. θ is the angle between the radial vector **r** and the y axis, as shown in Fig. 2.

We start by considering an arbitrary point (y,z) on the domain boundary. The radial vector **r** connecting the origin with this point can be decomposed into components normal and tangential to the local domain boundary with respective lengths L_n and L_t. We see from Fig. 2 that L_n and L_t can be expressed in terms of y and z as

$$L_n = y\cos\beta + z\sin\beta, \tag{1a}$$

$$L_t = y\sin\beta - z\cos\beta. \tag{1b}$$

The growth velocities in the normal and tangential directions are given by

$$v_n(\beta) = \frac{dL_n}{dt}, \tag{2a}$$

$$v_t(\beta) = \frac{dL_t}{dt}. \tag{2b}$$

Throughout this paper, we have assumed that the normal growth velocity, $v_n(\beta)$, is given. The tangential component may conveniently be expressed in terms of the normal velocity as

$$v_t(\beta) = -\frac{dv_n(\beta)}{d\beta}. \tag{3}$$

It is clear from the preceding equations that if the normal growth velocity $v_n(\beta)$ is independent of time t, then so are the tangential component $v_t(\beta)$ and the total velocity $v(\beta)$. The domain wall positions can be derived from L_n and L_t, which are found by a trivial integration to be

$$L_n(\beta,t) = v_n(\beta)t + L_n^0(\beta), \tag{4a}$$

$$L_t(\beta,t) = -\frac{dv_n(\beta)}{d\beta}t + L_t^0(\beta), \tag{4b}$$

where L_n^0 and L_t^0 are the initial values of L_n and L_t at $t=0$. The domain wall position may alternatively be written in terms of the polar coordinates (r,θ) in the form

$$r = \sqrt{[v_n(\beta)t + L_n^0(\beta)]^2 + \left(-\frac{dv_n(\beta)}{d\beta}t + L_t^0(\beta)\right)^2}, \tag{5a}$$

$$\tan(\beta-\theta) = \frac{-\frac{dv_n(\beta)}{d\beta}t + L_t^0(\beta)}{v_n(\beta)t + L_n^0(\beta)}. \tag{5b}$$

It is evident from the equations that the domain shape at short times depends strongly on the initial shape of the domain. At long times, the domain growth becomes self-similar and an equilibrium shape is approached. In the limit $t\to\infty$, the equations reduce to

$$r = \sqrt{v_n(\beta)^2 + \left(\frac{dv_n(\beta)}{d\beta}\right)^2}\,t, \tag{6a}$$

$$\tan(\beta-\theta) = -\frac{1}{v_n(\beta)}\frac{dv_n(\beta)}{d\beta}. \tag{6b}$$

In this limit the domain shape is determined only by the normal velocity profile $v_n(\beta)$, irrespective of the initial shape at $t=0$. Under conditions of similar growth, the domain shape does not change with time, and the domain wall velocity $v(\theta) = r(\theta,t)/t$ is independent of r along any given direction.

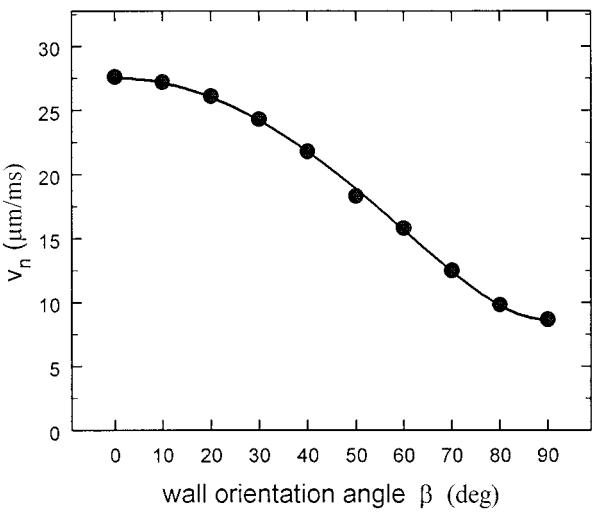

FIG. 3. Normal growth velocity profile $v_n(\beta)$ with the ratio of elastic constants $K_T/K_{BS} = 1/10$. The solid symbols represent the velocity obtained numerically. The curve is a fit of the form $v_n(\beta) \propto [K_T\sin^2(\beta) + K_{BS}\cos^2(\beta)]^{1/2}$, and is clearly in good agreement with the numerical result.

IV. FERROELECTRIC LIQUID CRYSTALS

In switching domain growth experiments, one would like to relate the observed normal velocity $v_n(\beta)$ to material properties of the system, as well as to the external field. In the case of field-driven domain growth in ferroelectric liquid crystals, we find that the Frank elastic constants play an important role in determining the growth velocities in different directions, and can be directly related to anisotropies in the domain shape. As a typical example, consider an SSFLC cell in an external electric field. The equation of motion describing the dynamics of director reorientation in chevron SSFLC cells can be written as [10]

$$\eta\frac{\partial\phi}{\partial t} = (K_{BS}\cos^2\beta + K_T\sin^2\beta)\frac{\partial^2\phi}{\partial y'^2} - PE\sin\phi\cos\delta - A\frac{\partial}{\partial\beta}\cos\chi, \tag{7}$$

where ϕ is the azimuthal angle of the director, K_{BS} and K_T are the Frank elastic constants for distortions of the director field, respectively, within and normal to the smectic layers, δ is the smectic layer tilt angle, E is the applied electric field, and P the spontaneous polarization. The last term describes orientational binding at the chevron interface, χ being the angle subtended between the directors immediately above and below the chevron interface, and A a material dependent parameter. The inclusion of a viscosity η implies a dissipative force damping azimuthal motion of the director. This formulation allows us to solve the 2D equation of motion for the special case of a 1D domain wall propagating along an arbitrary direction y' in the y-z plane.

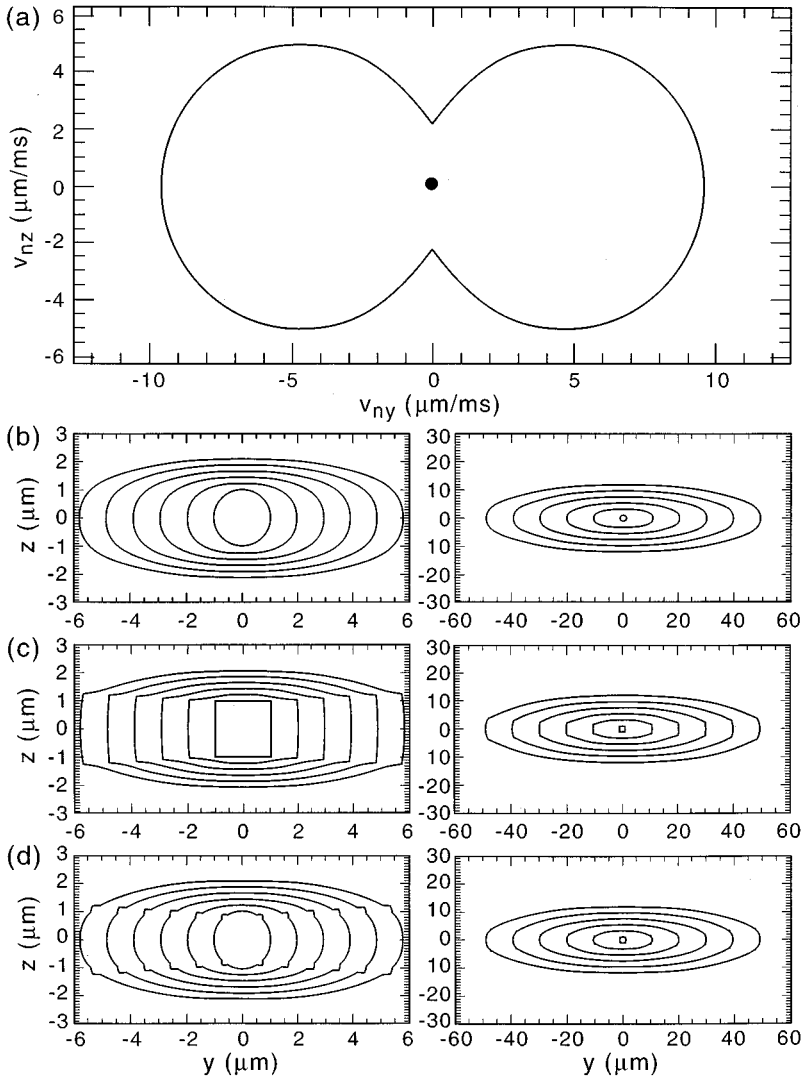

FIG. 4. (a) Computed angular dependence of the normal growth velocity $v_n(\beta)$ for a typical SSFLC cell in μm/ms. (b)–(d) Domain shape evolution for different nuclei: (b) circle, (c) square, and (d) circle with bumps. The early time evolution is depicted on the left at time intervals of 100 μs, while the long time growth is shown on the right using coarser time steps of 1 ms.

Comparing Eq. (7) with the standard sine-Gordon diffusion equation, and initially neglecting the chevron term for qualitative purposes, we can derive an effective orientational diffusion coefficient D_{eff} for very small ϕ,

$$D_{\text{eff}} \propto (K_{BS}\cos^2\beta + K_T \sin^2\beta)/\eta. \tag{8}$$

Alternatively, we can write $D_{\text{eff}} \sim v_n^2 \tau$, with v_n defined as before, and $\tau \sim \eta/(PE)$ the characteristic time derived from Eq. (7). Typically, τ has the order of 1 ms in our simulations. Substituting for D_{eff} in Eq. (8), we may obtain the dependence of the normal growth velocity on the external field, the elastic constants, the viscosity, as well as the polarization

$$v_n \propto \frac{\sqrt{PE}}{\eta}\sqrt{K_{BS}\cos^2\beta + K_T \sin^2\beta}. \tag{9}$$

This result implies that the velocity $v_n \propto \sqrt{E}$, consistent with earlier analytical and computational results [13]. We have performed numerical simulations in order to find the relation between the normal growth velocity and the related physical parameters, with the explicit inclusion of the chevron term. In this case, it is found that the normal velocity $v_n(\beta)$ has the form

$$v_n(\beta) \propto \frac{PE}{\eta}\sqrt{K_{BS}\cos^2\beta + K_T \sin^2\beta}, \tag{10}$$

i.e., $v_n(\beta)$ is found to be linear in E rather than proportional to $E^{1/2}$. This observed change of power law dependence of the growth velocity $v_n(\beta)$ on the field E must be due to the chevron term. The angular dependence of the normal velocity $v_n(\beta)$ arises in our model from the anisotropic properties of the Frank elastic constants, and does not depend on the chevron term. Velocity profiles $v_n(\beta)$ calculated from Eq. (7) are shown in Fig. 3. The calculated velocity profiles closely match the shape predicted by Eq. (10).

V. RESULTS

We have modeled the domain shape evolution of SSFLC's in the presence of an electric field using the method described above. The system is well-behaved, in the sense that the asymptotic form of the growing domain does not depend on its initial shape. For any given set of physical parameters, both polygonal and elliptical domain nuclei with either smooth or rough boundaries all evolve within a few characteristic times τ to the same smooth, elongated form.

Assigning different values to the elastic constants K_T and K_{BS} corresponding to the twist and bend-splay distortions of **P**, in accord with what is known of SC phases, is found to be an essential condition for generating anisotropic growth in the y-z plane. In addition, our simulations are the first to produce partial faceting similar to what is observed experimentally.

The evolution of some domain shapes computed by solving Eq. (5) starting from different initial configurations but with the same normal velocity profile $v_n(\beta)$ are shown in Fig. 4. Figure 4(a) shows the velocity profile $v_n(\beta)$ computed by solving Eq. (7), with $K_T/K_{BS}=1/10$. It can be seen from Fig. 4(a) that the profile of the velocity is smooth except for two singularities located at $\beta=\pi/2$ and $3\pi/2$. The Wulff construction would predict that the cusps in $v_n(\beta)$ should produce the facets of the domain wall. Figure 4(b) shows the domain shape at different times when the initial nucleus is circular. It is found at early times that the local wall orientation β along any radial direction θ varies with time, implying that the domain growth is not initially self-similar. At long times, however, the equilibrium shape determined by the velocity profile $v_n(\beta)$ is approached. The equilibrium domain shape has facets corresponding to the cusps of the velocity profile. Figure 4(c) shows the evolution of an initially square nucleus. At first we find that those parts of the domain boundary with orientations close to the cusps in $v_n(\beta)$ evolve most rapidly, while keeping the other parts unchanged. Although the sharp corners are rounded relatively slowly, the final shape is still the same as in Fig. 4(b). We also watched the evolution of a circle with some pointed bumps on it, shown in Fig. 4(d). Although the absolute height of the bumps does not change with time, the bumps in this example become negligibly small in comparison with the domain size as time goes on.

Faceting in this model is a combined consequence of the elastic anisotropy and the chevron potential. The domain wall velocity is smaller along the layer normal $\hat{\mathbf{z}}$ than along the layers themselves because $K_T<K_{BS}$, causing a cusp in the velocity diagram at $\beta=\pi/2$ that is in turn responsible for faceting. The chevron binding term introduces an energy barrier that further slows down wall motion, deepening the cusps in $v_n(\beta)$.

Finally, we also performed simulations for the arbitrary velocity profile shown in Fig. 5(a). This angular dependence of the growth velocity $v_n(\beta)$ does not arise from our SSFLC model. Since there are four cusps in the velocity profile, we would predict that the equilibrium shape of the domain is a rectangle. The evolution of domain shape with time for a circular nucleus and for a circular nucleus with some bumps on it are displayed, respectively, in Figs. 5(b) and 5(c). We see that within a very short time, the equilibrium form, a rectangle, is indeed reached. In particular, we note in Fig. 5(c) that when the nucleus begins to grow outward, the bumps are first expanded into facets, which become wider and wider until they form the sides of the rectangle.

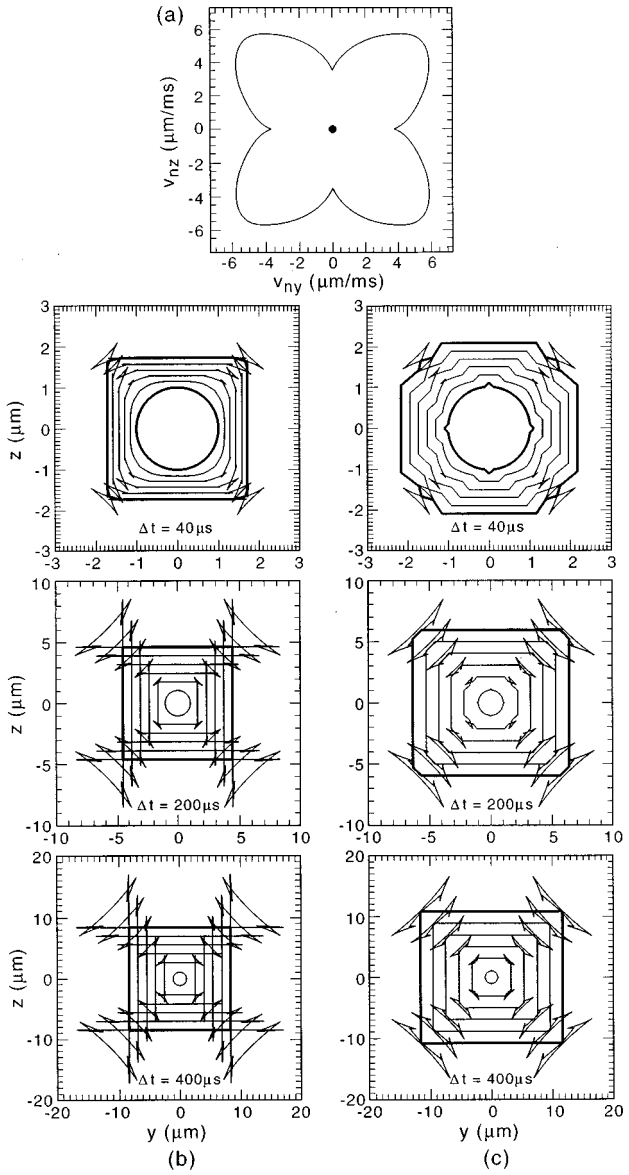

FIG. 5. Domain growth for an arbitrary velocity profile. (a) Growth velocity $v_n(\beta)$ in μm/ms; (b) growth from a circular nucleus; (c) growth from a circular nucleus with bumps on it. The evolution in each frame starts from the same initial domain shape at $t=0$. Successive vertical frames show the evolution over different time scales. The ''swallow tails'' are typical artifacts of these calculations: the actual domain shapes for selected times are emphasized with thicker lines.

VI. DISCUSSION

In our simulations we have considered the growth of a single domain from an isolated nucleus. By introducing anisotropy in the elastic constants, domain growth is seen to occur more rapidly along the layers than perpendicular to them. Including a chevron binding potential leads to a flattening of the sides of the domain. However, there is evidently nothing in the present model to cause further faceting or asymmetric growth in the layer direction.

Experimentally, we observed several hitherto unexplained variations in SSFLC domain shape, such as the transitions from rounded to faceted domain boundaries, and from asymmetric pentagonal (''boat'') shapes to elongated hexagons, both dependent on the applied field strength. This implies that the angular dependence of normal growth velocity $v_n(\beta)$ is determined not only by the anisotropic elastic

properties of the material, but also by the external field. Our present growth model does not account for these phenomena and it is thought that flow effects may need to be included [9].

The Wulff construction is a very simple way of determining the equilibrium shapes of crystals using the anisotropic surface tension. This is especially true for a crystal, whose shape turns out to be rigorously polyhedral due to its rigidity. Thus the smooth angular dependence of surface tension $\gamma(\beta)$ on outnormal angle β effectively reduces to an array of discrete points, i.e., the cusped minima of $\gamma(\beta)$ suffice to define the domain shape. In this case the Wulff construction is more effective and more precise than the present method used here. However, if we expect to consider the equilibrium shape of partially ordered materials, such as liquid crystals or a hexatic phase in a melting transition, where the dependence of surface tension or elastic coefficients on the surface normal is continuous and single-valued, our analytical procedure gives the domain shape in a very straightforward way.

VII. CONCLUSION

In summary, we have developed a generally analytical method which can be used to evaluate the evolution of domain shapes with time. It has been shown that the equilibrium shape of the domain is only determined by the normal growth velocity profile $v_n(\beta)$, no matter what the initial shape is. A connection between the normal growth velocity $v_n(\beta)$ and the effective elastic constant $K(\beta)$ in chevron SSFLC's has been established, allowing the equilibrium shape to be related to the inherent properties of the material. A systematic comparison of experimental and numerical data should therefore enable the determination of some important physical parameters. For example, an inversion of the present method here should yield the ratio of the Frank elastic constants in different directions. Measurements of threshold fields and switching times may yield an estimate of the chevron binding energy, A. All of these will be very interesting topics for future study.

ACKNOWLEDGMENTS

This work was supported by NSF Grants No. EEC 90-15128 and No. DMR 92-24168, and by ARO Contract No. DAA H04-93-G0164.

[1] M. Seul and D. Andelman, Science **267**, 476 (1995).
[2] G. Wulff, Z. Krist. **34**, 449 (1901).
[3] R. B. Meyer, L. Liebert, L. Strzelecki, and P. Keller, J. Phys. (Paris) Lett. **36**, L69 (1975).
[4] N. A. Clark and S. T. Lagerwall, Appl. Phys. Lett. **36**, 899 (1980).
[5] T. P. Rieker, N. A. Clark, G. S. Smith, D. S. Parmar, E. B. Sirota, and C. R. Safinya, Phys. Rev. Lett. **59**, 2658 (1987).
[6] J. E. Maclennan, M. A. Handschy, and N. A. Clark, Liq. Cryst. **7**, 787 (1990).
[7] J. E. Maclennan, N. A. Clark, M. A. Handschy, and M. R. Meadows, Liq. Cryst. **7**, 753 (1990); Z. Zhuang, N. A. Clark, and J. E. Maclennan, *ibid.* **10**, 409 (1991).
[8] M. A. Handschy and N. A. Clark, Appl. Phys. Lett. **41**, 39 (1982).
[9] J.-Z. Xue and N. A. Clark, Phys. Rev. E **48**, 2043 (1993).
[10] J. E. Maclennan, Q. Jiang, and N. A. Clark, Phys. Rev. E **52**, 3904 (1995).
[11] C. Herring, Phys. Rev. **82**, 87 (1951); C. Herring, in *Structure and Properties of Solid Surfaces*, edited by R. Gomer and C. Smith (University of Chicago Press, Chicago, 1953).
[12] M. A. Handschy and N. A. Clark, Ferroelectrics **59**, 69 (1984).
[13] J. E. Maclennan, M. A. Handschy, and N. A. Clark, Phys. Rev. A **34**, 3554 (1986).